# Element partitioning and diffusion in natural grains

*Submitted By*

**Chandan Kumar Sahu**

School of Physical Sciences

National Institute of Science, Education and Research (NISER), Bhubaneswar

*Under the Guidance of*

**Dr. Subhasis Basak**

**Reader-F**

School of Physical Sciences

National Institute of Science, Education and Research (NISER), Bhubaneswar


*Supervised by*

**Dr. Priyadarshi Chowdhury**

**Assitant professor**

School of Earth and Planetary Sciences

National Institute of Science, Education and Research (NISER), Bhubaneswar

# Element partitioning and diffusion in natural grains

**Abstract:** *Interdiffusion within olivine represents a extensively researched phenomenon pivotal for understanding element partitioning and facilitating time-series analysis, particularly in the determination of diffusion coefficients and associated time-series studies. Such investigations find widespread application in geochronological studies. This report begins with an exploration of fundamental principles of Fickian diffusion, followed by the examination of heat diffusion within simplified systems. Subsequently, we undertake modeling of Fe-Mg interdiffusion in fosterite, aiming to ascertain diffusion coefficients through examination of laboratory-grown samples, thereby validating the diffusion model. Employing an Arrhenius fit, we derive activation energies for the olivine samples. Finally, leveraging this model, we compute the total elapsed diffusion time for natural grains sourced from volcanic eruptions, thereby probing the duration between the volcano's active stage at specific pressure levels and the eruption event.*

## 1 Introduction

Olivine, a prevalent silicate mineral, holds a significant presence in various rocks, spanning from surface volcanoes on both landmasses and ocean floors to the profound layers of the Earth's mantle. Moreover, it plays a vital role in many extraterrestrial silicate specimens sourced from celestial bodies such as the moon, Mars, and asteroids [7]. This extensive distribution owes to olivine's broad thermodynamic stability, uncomplicated chemical composition, and structural characteristics. [1].

The rate of Fe-Mg interdiffusion in olivine holds significance in several aspects. It influences the determination of closure temperatures for different ion exchange geothermometers, aids in calculating cooling rates and other thermal history details via compositional zoning profiles, and contributes to understanding the point defect chemistry within olivines. Moreover, these interdiffusion rates serve as a basis for interpreting data related to other transport properties of olivine, including creep rates and electrical conductivity [4, 5].

The chemical formula for olivine is $(Mg,Fe)_2SiO_4$, reflecting its composition primarily of Magnesium (Mg), Iron (Fe), silicon (Si), and oxygen (O). It crystallizes in the orthorhombic system, forming distinctive green crystals. Olivine is commonly found in igneous rocks such as basalt and gabbro and is also a component of the Earth's mantle. Its high density and hardness contribute to its durability in geological processes.

## 2 The Diffusion Equation

Diffusion is the spontaneous movement of particles, atoms, or molecules from regions of higher concentration to regions of lower concentration, driven by random thermal motion. The Fickian diffusion governs grain interdiffusion within crystalline structures, describing the gradual movement of atoms between adjacent grains driven by concentration gradients. In this mechanism, atoms migrate through lattice vacancies or interstitial sites, following Fick's first law of diffusion. The rate of diffusion depends on factors such as temperature, atomic size, and the presence of defects. In the case of grains, two elemental/mineral concentrations mix with each other through diffusion at high temperatures. Understanding Fickian diffusion in grain interdiffusion is crucial for elucidating processes like phase transformations, solid-state reactions, and the evolution of microstructures in materials science and engineering contexts.

The basic form of the diffusion equation can be given by

$$\frac{\partial C}{\partial t} = \frac{\partial}{\partial x}\left(D\frac{\partial C}{\partial x}\right) \tag{1}$$

where $C$ is the concentration of the grain, $x$ is the length of the grain, and t is the time. If the diffusion coefficient is independent of the length, then the equation becomes

$$\frac{\partial C}{\partial t} = D\frac{\partial^2 C}{\partial x^2} \tag{2}$$

This report aims to model the interdiffusion in forsterite mineral grains, i.e., Fe-Mg grains, to determine their concentration variation over time. We will also compare them with experimentally obtained datasets and check the goodness of our model. Finally, we will also use this knowledge to obtain the time evolution of grain in natural systems, i.e., grains obtained from actual volcano eruptions, and understand when the volcano became active.

## 3 1-D Heat Diffusion in Metal Rods

Before moving into the modeling details, let us model the diffusion first. We will begin with the simple examples from heat diffusion to set up the basis, then move towards the application to complex grain systems.

### 3.1 Methodology - Finite Difference Forward Euler

We use the simplest method of all, the forward difference method, using the forward Euler method to solve the diffusion equation. In this method, the diffusion equation is discretized based on a simple discretization scheme.

$$\frac{\partial T}{\partial t} \approx \frac{T^{j+1} - T^j}{dt} \tag{3}$$

where $dt$ is the the time-step size and $T^j$ is the temperature at the $j^{th}$ time-step. Similarly, the derivative and double derivative in spatial coordinates can also be defined as $dx$ is the spatial-step size and $T_i$ is the temperature at the $i^{th}$ spatial step.

$$\frac{\partial T}{\partial x} \approx \frac{T_{i+1} - T_i}{dx} \tag{4}$$

$$\frac{\partial^2 T}{\partial x^2} \approx \frac{T_{i+1} - 2T_i + T_{i-1}}{dx^2} \tag{5}$$

Together, the diffusion equation 2 becomes

$$\frac{T_i^{j+1} - T_i^j}{dt} = D \left( \frac{T_{i+1}^j - 2T_i^j + T_{i-1}^j}{dx^2} \right) \tag{6}$$

We solved this iteratively using Python and obtained the solutions. Let us explore some examples to understand how it works.

## 3.2 Heat diffusion in one metal rod

### 3.2.1 Example 1 - A metal rod with both ends at fixed temperatures

Consider a metal rod with length=1 m heated in a furnace up to a temperature of 1000 K and then kept in contact with two furnaces of 500 K and 100 K temperatures, respectively. The evolution of the temperature of the rod is then observed. Table 1 shows the run parameters. Fig. 1 shows a contour plot showing the heat diffusion.

Table 1: Parameters for example 1

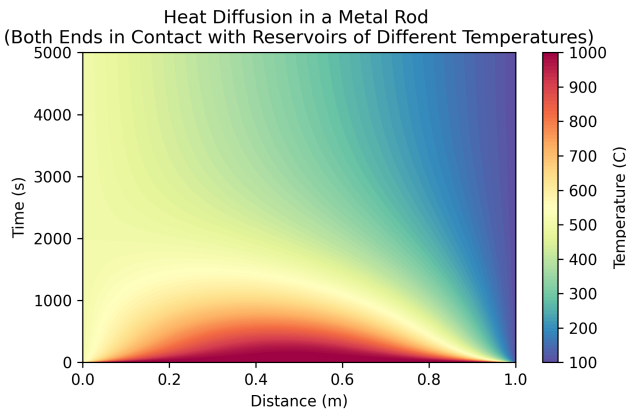| Parameters | Values |
|---|---|
| length of rod | $1\ m$ |
| evolution time | $5000\ s$ |
| $dt$ | $0.1\ s$ |
| $dx$ | $0.01\ m$ |
| $D$ | $10^{-4}\ m^2/s$ |
| $T_{\text{initial}}$ | 1000 K |
| $T_{\text{left}}$ | 500 K |
| $T_{\text{right}}$ | 100 K |



Figure 1: *Heat diffusion of a metal rod with both ends at fixed temperatures*

### 3.2.2 Example 2 - A metal rod with one end at fixed temperature and the other end insulated

Consider a metal rod with length=1 m heated in a furnace up to a temperature of 1000 K, and then one of its ends is kept in contact with a furnace of temperatures 400 K, and the other end is insulated. The evolution of the temperature of the rod is then observed. Table 2 shows the run parameters. Fig. 2 shows a contour plot showing the heat diffusion.

Table 2: Parameters for example 1

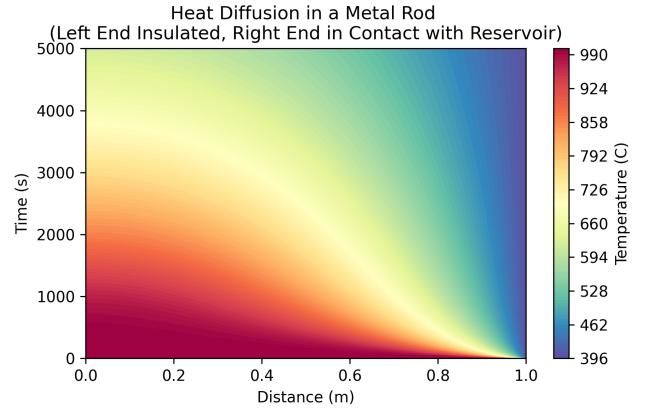| Parameters | Values |
|---|---|
| length of rod | $1\ m$ |
| evolution time | $5000\ s$ |
| $dt$ | $0.1\ s$ |
| $dx$ | $0.01\ m$ |
| $D$ | $10^{-4}\ m^2/s$ |
| $T_{\text{initial}}$ | 1000 K |
| $T_{\text{right}}$ | 400 K |



Figure 2: *Heat diffusion of a metal rod with one end insulated*

## 3.3 Heat diffusion in two joint metal rods

### 3.3.1 Example 3 - Two metal rods joined together

Consider two metal rods of different kinds (different diffusion coefficients) with length=1 m, each heated in a furnace up to a temperature profile of $T_1^{\text{initial}}$ and $T_2^{\text{initial}}$ given by eqn. 7 and 8.

$$T_1^{\text{initial}} = -800(x - 0.5)^2 + 1000 \tag{7}$$

$$T_2^{\text{initial}} = -600(x - 1.5)^2 + 600 \tag{8}$$

These are then joined together, keeping their extreme ends insulated. The evolution of the temperature of the rod is then observed. Table 3 shows the run parameters. Fig. 3 shows a contour plot showing the heat diffusion.

| Table 3: Parameters for example 1 | |
|---|---|
| Parameters | Values |
| length of rod 1 | $1\ m$ |
| length of rod 2 | $1\ m$ |
| evolution time | $5000\ s$ |
| $dt$ | $0.1\ s$ |
| $dx$ | $0.05\ m$ |
| $D_1$ | $5 \times 10^{-4}\ m^2/s$ |
| $D_2$ | $10^{-4}\ m^2/s$ |

| Table 4: Parameters for example 1 | |
|---|---|
| Parameters | Values |
| length of rod 1 | $1\ m$ |
| length of rod 2 | $1\ m$ |
| evolution time | $10000\ s$ |
| $dt$ | $0.1\ s$ |
| $dx$ | $0.05\ m$ |
| $D_1$ | $5 \times 10^{-4}\ m^2/s$ |
| $D_2$ | $10^{-4}\ m^2/s$ |
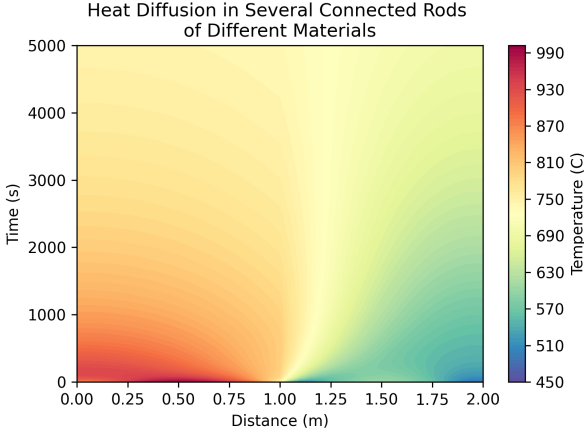


Figure 3: *Heat diffusion of two joint metal rods of different kinds.*
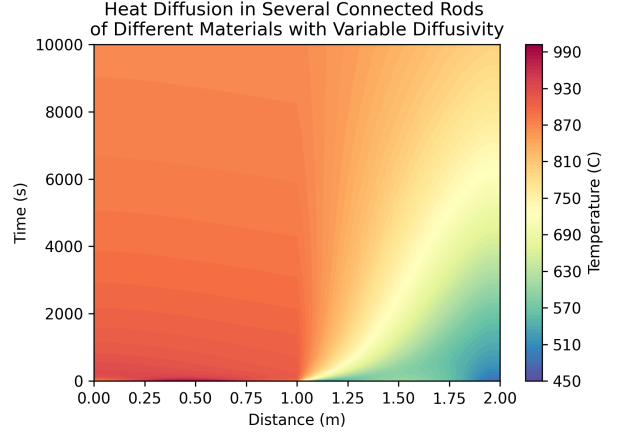


Figure 4: *Heat diffusion of two joint metal rods of different kinds and varying diffusion coefficient.*

### 3.3.2 Example 4 - Two metal rods with varying diffusion coefficients joined together

Consider two metal rods of different kinds (different diffusion coefficients, and these vary with length) with length=1 m, each heated in a furnace up temperature profiles of $T_1^{\text{initial}}$ and $T_2^{\text{initial}}$ are given by eqn. 9 and 10. Additionally, their diffusion coefficients $D_1$ and $D_2$, and thermal conductivities $k_1$ and $k_2$ are given by eqn. 11, 12, 13 and 14 respectively. The diffusion is governed by 1 instead of 2.

$$T_1^{\text{initial}} = -800(x - 0.5)^2 + 1000 \tag{9}$$

$$T_2^{\text{initial}} = -600(x - 1.5)^2 + 600 \tag{10}$$

$$D_1 = 10^{-3}x + 10^{-4} \tag{11}$$

$$D_2 = 9 \times 10^{-4}(1 - x) + 10^{-3} \tag{12}$$

$$k_1 = 10^{-3}x + 10^{-4} \tag{13}$$

$$k_2 = 9 \times 10^{-4}(1 - x) + 10^{-3} \tag{14}$$

These are then joined together, keeping their extreme ends insulated. The evolution of the temperature of the rod is then observed. Table 4 shows the run parameters. Fig. 4 shows a contour plot showing the heat diffusion.

The stability of the explicit Euler method is governed by the Courant–Friedrichs–Lewy condition or the CFL condition, which states that

$$D\frac{dt}{dz^2} \leq 0.5 \tag{15}$$

This has the disadvantage of instability at a higher diffusion coefficient, which can be removed at the cost of high computation power. To overcome this, implicit schemes were developed, using the information from the previous and present time steps to obtain values at the present time-step. The entire code for this part of the project can be found in the `"Heat diffusion in metal rods"` folder of ://github.com/chandan-kumarsahu/CP-Project-Grain-Interdiffusion/.

With the introduction of the semi-implicit Crank-Nicholson scheme, we move to the grain diffusion problem statement.

## 4 Interdiffusion of grain concentration in forsterite

forsterite is a common mineral belonging to the olivine group, with the chemical formula $Mg_2SiO_4$. It typically occurs in metamorphic rocks and is often associated with minerals like forsterite, fayalite, and peridotite. Forsterite is characterized by its pale green color and translucent to transparent appearance.

The interdiffusion of Iron and Magnesium in forsterite plays a significant role in various geological and material

science contexts. Iron (Fe) and Magnesium (Mg) are two essential components of forsterite, and their interdiffusion affects the mineral's properties, such as thermal and electrical conductivity. Understanding the kinetics and mechanisms of iron-magnesium interdiffusion in forsterite is crucial for interpreting geological processes like metamorphism and deformation in rocks containing this mineral. Moreover, it has implications for material engineering applications, particularly in understanding diffusion processes in high-temperature materials and ceramics.
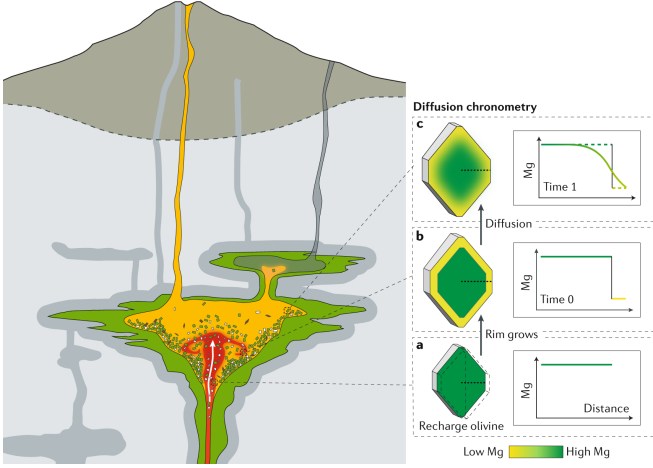


Figure 5: Interdiffusion of forsterite [3]

As the temperature rises, the kinetic energy of the atoms increases, allowing them to overcome energy barriers and migrate through the crystal lattice. This interdiffusion primarily involves the exchange of Magnesium (Mg) and Iron (Fe) atoms, as they are the most abundant elements within the mineral. Iron atoms, typically present in trace amounts in forsterite, diffuse into the lattice and replace magnesium atoms, forming solid solutions known as the series of olivine minerals. The rate of interdiffusion is influenced by factors such as temperature, pressure, and the concentration gradient of Iron and Magnesium within the mineral. Higher temperatures favor faster interdiffusion rates, resulting in a more homogenized distribution of Iron and Magnesium within the forsterite crystal lattice.

In this section, we apply the diffusion equation to study the interdiffusion of Mg and Fe in forsterite. We will first use laboratory-prepared grains of olivine samples that have undergone diffusion at a specific temperature at a particular time to obtain the diffusion coefficient.

In the following section, we will use this knowledge and estimate the time since the diffusion started in some naturally obtained samples of forsterite from volcanic eruptions to estimate the period since when the volcano was active before erupting. This will enable us to understand the normal time period of volcanic activity and make better predictions in the future.

## 4.1 Methodology - Crank-Nicholson scheme

Due to stability issues, using implicit or semi-implicit solver schemes is more convenient. Here, we use the Crank-Nicholson semi-implicit scheme to solve the diffusion equation numerically. The Crank-Nicholson method is very efficient in solving partial differential equations, particularly those describing the diffusion of heat or mass transfer. It is a powerful approach that combines implicit and explicit methods, providing stability and accuracy in solving time-dependent problems. By averaging values at current and future time steps, Crank-Nicholson strikes a balance between computational efficiency and numerical stability, making it widely used in various fields such as computational fluid dynamics, heat transfer analysis, and quantum mechanics simulations.

We begin by discretizing the diffusion equation given in eqn. 2

$$\frac{C_i^{j+1} - C_i^j}{dt} = \frac{D}{2} \left( \frac{C_{i+1}^{j+1} - 2C_i^{j+1} + C_{i-1}^{j+1}}{dz^2} \right) \tag{16}$$

$$+ \frac{D}{2} \left( \frac{C_{i+1}^j - 2C_i^j + C_{i-1}^j}{dz^2} \right) \tag{17}$$

Now we separate the present time-step $(j+1)$ and the past time-step $(j)$

$$C_i^{j+1} - \frac{D\,dt}{2\,dz^2} \left( C_{i+1}^{j+1} - 2C_i^{j+1} + C_{i-1}^{j+1} \right) = \tag{18}$$

$$C_i^j + \frac{D\,dt}{2\,dz^2} \left( C_{i+1}^j - 2C_i^j + C_{i-1}^j \right) \tag{19}$$

Taking $\frac{D\,dt}{2\,dz^2} = \sigma$, we rewrite the equations as

$$(1 + 2\sigma)\,C_i^{j+1} - \sigma C_{i+1}^{j+1} - \sigma C_{i-1}^{j+1} = \tag{20}$$

$$(1 - 2\sigma)\,C_i^j + \sigma C_{i+1}^j + \sigma C_{i-1}^j \tag{21}$$

We can now form a matrix for the two time-steps and solve it.

$$MC^{j+1} = NC^j$$

where

$$M = \begin{bmatrix} 1+2\sigma & -\sigma & 0 & \cdots & 0 \\ -\sigma & 1+2\sigma & -\sigma & \ddots & \vdots \\ 0 & -\sigma & 1+2\sigma & \ddots & 0 \\ \vdots & \ddots & \ddots & \ddots & -\sigma \\ 0 & \cdots & 0 & -\sigma & 1+2\sigma \end{bmatrix} \tag{22}$$

$$\tag{23}$$

$$N = \begin{bmatrix} 1-2\sigma & \sigma & 0 & \cdots & 0 \\ \sigma & 1-2\sigma & \sigma & \ddots & \vdots \\ 0 & \sigma & 1-2\sigma & \ddots & 0 \\ \vdots & \ddots & \ddots & \ddots & \sigma \\ 0 & \cdots & 0 & \sigma & 1-2\sigma \end{bmatrix} \tag{24}$$

It is noteworthy that vacuum boundary conditions have been considered in this demonstration. For the case

of isolated boundary conditions, the discretized solution has to be solved separately at the boundaries and then applied to the matrices. The final answer i.e., $T^{j+1}$ is obtained as

$$C^{j+1} = M^{-1}NC^j \tag{25}$$

This solution, however, is the basic form of the Crank-Nicholson method. We modify the scheme according to our needs as follows. As shown in Fig. 5, the Fe atoms are initially outside the compartment, maintaining a natural partition. When temperature increases, the Fe atoms diffuse into the Mg partition, and Mg diffuses into the Fe partition. This leads to taking two separate compartments for Fe and Mg and then modifying the boundary conditions to incorporate diffusion. Moreover, the boundaries considered for our case of grain interdiffusion are isolated boundary conditions.

## 4.2 Calculating the diffusion coefficient from lab samples

This section will calculate the diffusion coefficient of Fe-Mg forsterite laboratory-grown samples collected from [1]. We use 4 sample data: OLID 8, OLID 9, OLID 10 and OLID 202. The data files and entire code can be found in the `Element Partitioning and Diffusion` folder of https://github.com/chandan-kumarsahu/CP-Project-Grain-Interdiffusion/

### 4.2.1 OLID 10 dataset

Table 5: Parameters for OLID 10 dataset [1].

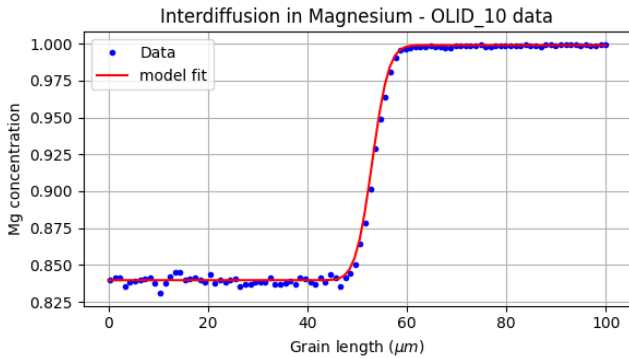| Parameters | Values |
|---|---|
| Total length of grain | $101\mu m$ |
| $L_1$ (pure Mg side) | $46.5\mu m$ |
| $L_2$ (Fe-Mg mixed side) | $54.5\mu m$ |
| Total time | 360 hrs |
| $dt$ | 0.5 hrs |
| $dx$ | $1\mu m$ |
| Length offset | $201\mu m$ |
| Temperature | $1000\ ^{\circ}C$ |
| $\log[f(O_2)]$ | -11.97 bars |



Figure 6: Variation of concentration of Magnesium with grain length in sample OLID 10

We perform a Root Mean Square Error analysis (RMSE) on the dataset to match our model and obtain the best-fit value for the diffusion coefficient. From table 5 and Fig. 6, we obtain the diffusion coefficient

$$D_{\text{OLID 10}} = (2.842 \pm 0.666) \times 10^{-18} m^2/s$$

### 4.2.2 OLID 8 dataset

Table 6: Parameters for OLID 8 dataset [1].

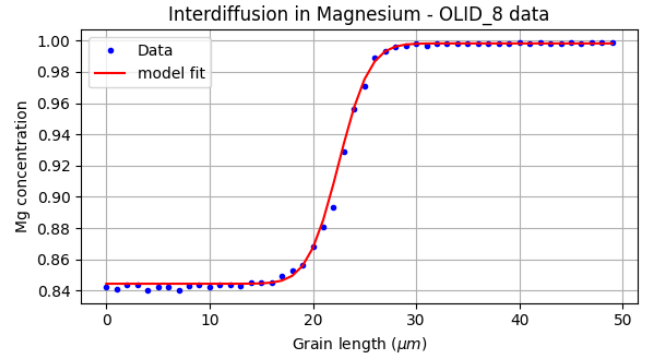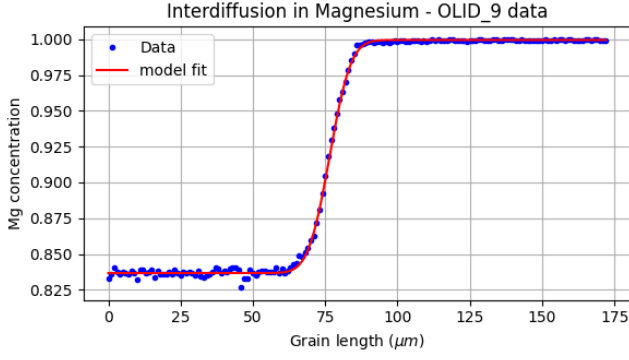| Parameters | Values |
|---|---|
| Total length of grain | $50\mu m$ |
| $L_1$ (pure Mg side) | $26.5\mu m$ |
| $L_2$ (Fe-Mg mixed side) | $23.5\mu m$ |
| Total time | 164 hrs |
| $dt$ | 0.5 hrs |
| $dx$ | $1\mu m$ |
| Length offset | $0\mu m$ |
| Temperature | $1100\ ^{\circ}C$ |
| $\log[f(O_2)]$ | -12.02 bars |



Figure 7: Variation of concentration of Magnesium with grain length in sample OLID 8

From table 6 and Fig. 7, we obtain the diffusion coefficient

$$D_{\text{OLID 8}} = (5.117 \pm 0.799) \times 10^{-18} m^2/s$$

### 4.2.3 OLID 9 dataset

Table 7: Parameters for OLID 9 dataset [1].

| Parameters | Values |
|---|---|
| Total length of grain | $173\mu m$ |
| $L_1$ (pure Mg side) | $96\mu m$ |
| $L_2$ (Fe-Mg mixed side) | $77\mu m$ |
| Total time | 117 hrs |
| $dt$ | 0.5 hrs |
| $dx$ | $1\mu m$ |
| Length offset | $0\mu m$ |
| Temperature | $1200\ ^{\circ}C$ |
| $\log[f(O_2)]$ | -11.98 bars |

Figure 8: Variation of concentration of Magnesium with grain length in sample OLID 9

From table 7 and Fig. 8, we obtain the diffusion coefficient

$$D_{\text{OLID 9}} = (4.052 \pm 0.053) \times 10^{-17} m^2/s$$

#### 4.2.4 OLID 202 dataset

Table 8: Parameters for OLID 202 dataset [1].

| Parameters | Values |
|---|---|
| Total length of grain | $188\mu m$ |
| $L_1$ (pure Mg side) | $83\mu m$ |
| $L_2$ (Fe-Mg mixed side) | $105\mu m$ |
| Total time | 52.4 hrs |
| $dt$ | 0.5 hrs |
| $dx$ | $1\mu m$ |
| Length offset | $0\mu m$ |
| Temperature | 1300 $^\circ C$ |
| $\log[f(O_2)]$ | -12.04 bars |
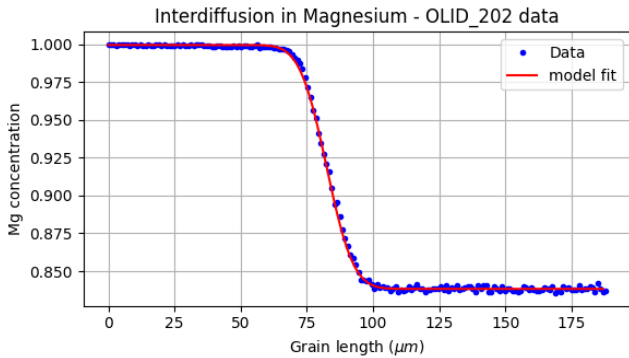


Figure 9: Variation of concentration of Magnesium with grain length in sample OLID 202

From table 8 and Fig. 9, we obtain the diffusion coefficient

$$D_{\text{OLID 202}} = (1.721 \pm 0.004) \times 10^{-16} m^2/s$$

The diffusion coefficient increases with temperature

governed by the Arrhenius equation

$$D = D_0 \exp\left(-\frac{Q}{RT}\right) \qquad (26)$$

where $D_0$ is the diffusion coefficient at zero temperature, $Q$ is the activation energy and $R$ is the gas constant.

We will fit the data points from all the samples to obtain the values of $Q$ and $D_0$.

$$\ln D = \ln D_0 - \frac{Q}{RT} \qquad (27)$$

$$\text{or} \qquad y = c + mx \qquad (28)$$

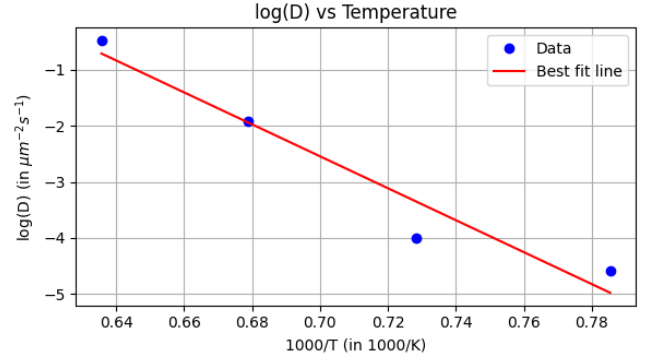where $x = 1/T$, $y = \ln D$, $m = -Q/R$ and $c = \ln D_0$.



Figure 10: Straight line fitting of diffusion coefficients on Arrhenius equation, datasets from OLID 8, OLID 9, OLID 10, and OLID 202

Fig. 10 represents a straight line fitting over the obtained diffusion coefficients. From this, we obtain the values of $Q$ and $D_0$ as

$$Q = 236.641 \text{ kJ/mol}$$

$$D_0 = 9.81 \times 10^{-9} m^2/s$$

We use the Pearson coefficient to measure the goodness of fit, which was found to be 0.9703, describing a decent fit. The final fit has been shown in Fig. 11.
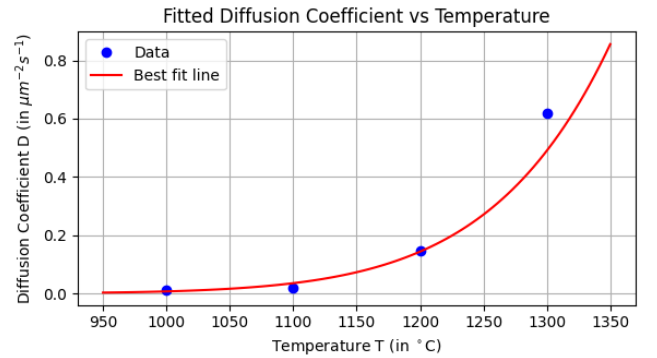


Figure 11: Fitted Arrhenius curve

We conclude that our diffusion model agrees well with the observed data from [1] and explains the interdiffusion of Fe-Mg element partitioning very well.

## 4.3 Obtaining the diffusion time from natural volcanic grains

We now work with actual samples collected from the Mt. Etna volcano, which erupted on April 11, 2007, and another volcano in San Pedro, Chile. In this subsection, we use the three samples, namely Ol6a, Ol6b, and SanPedro datasets. The data files and entire code can be found in the `Element Partitioning and Diffusion` folder of https://github.com/chandan-kumarsahu/CP-Project-Grain-Interdiffusion/

In this case, the diffusion coefficients are calculated separately using the following formula [5]

$$\log\left(D^c_{\text{Fe-Mg}}\right) = -\frac{201000 + (P - 10^5) \cdot 7 \cdot 10^{-6}}{2.303 \cdot R \cdot T} \tag{29}$$

$$+ \frac{1}{6} \cdot \log(fO_2/10^{-7}) \tag{30}$$

$$+ 3 \cdot (X_{\text{Fe}} - 0.1) - 9.21 \tag{31}$$

where $D^c_{\text{Fe-Mg}}$ is in $m^2/s$, $T$ is in $K$, $P$ and $fO_2$ are in pascals and $X_{\text{Fe}}$ is equivalent to the molar fraction of fayalite or Iron in the olivine sample.

### 4.3.1 Ol6a dataset

Table 9: Parameters for Ol6a dataset [4, 5].

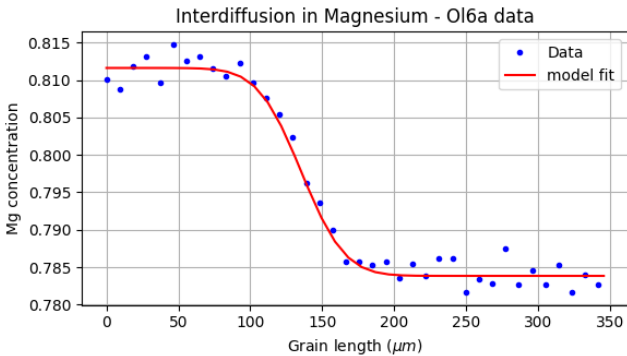| Parameters | Values |
| --- | --- |
| Total length of grain | $355\mu m$ |
| $L_1$ (Mg side) | $143\mu m$ |
| $L_2$ (Fe-Mg mixed side) | $212\mu m$ |
| $dt$ | 5 hrs |
| $dx$ | $1\mu m$ |
| Length offset | $46\mu m$ |
| Temperature | 1083 $°C$ |
| $\log[f(O_2)]$ | -9.02292 bars |
| Pressure | $2 \times 10^8$ bars |
| $X_{\text{Fe}}$ | 0.2 |



Figure 12: Variation of concentration of Magnesium with grain length in natural sample Ol6a

Feeding in the values from table 9, the diffusion coefficient was found to be

$$D_{\text{Ol6a}} = 6.1875 \times 10^{-17} m^2/s$$

Again, we perform a root mean square error analysis (RMSE) on the dataset to match our model and obtain the best-fit value for the diffusion time. From table 9 and Fig. 12, we obtain the diffusion time

$$t_{\text{Ol6a}} = 56.4583 \pm 0.0001 \text{ days}$$

### 4.3.2 Ol6b dataset

Table 10: Parameters for Ol6b dataset [4, 5].

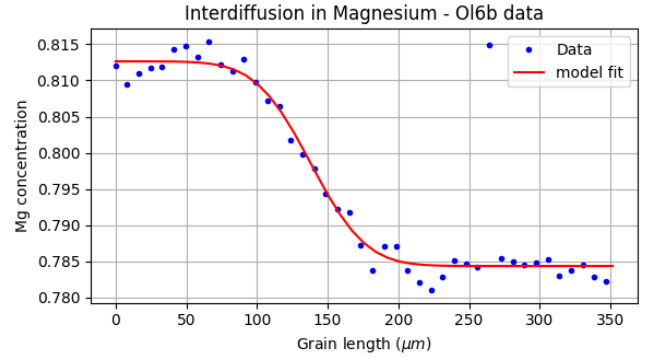| Parameters | Values |
| --- | --- |
| Total length of grain | $360\mu m$ |
| $L_1$ (Mg side) | $143\mu m$ |
| $L_2$ (Fe-Mg mixed side) | $217\mu m$ |
| $dt$ | 5 hrs |
| $dx$ | $1\mu m$ |
| Length offset | $58\mu m$ |
| Temperature | 1083 $°C$ |
| $\log[f(O_2)]$ | -9.02292 bars |
| Pressure | $2 \times 10^8$ bars |
| $X_{\text{Fe}}$ | 0.2 |



Figure 13: Variation of concentration of Magnesium with grain length in natural sample Ol6b

Feeding in the values from table 10, the diffusion coefficient was found to be

$$D_{\text{Ol6b}} = 6.1875 \times 10^{-17} m^2/s$$

Again, we perform a root mean square error analysis (RMSE) on the dataset to match our model and obtain the best-fit value for the diffusion time. From table 10 and Fig. 13, we obtain the diffusion time

$$t_{\text{Ol6b}} = 91.0417 \pm 0.0002 \text{ days}$$

### 4.3.3 SanPedro dataset

The San Pedro dataset shows poor quality, likely due to prolonged diffusion time hindering efficient interdiffusion. Additionally, data precision at the pure end is subpar. Therefore, we model only up to $300\mu m$ of the dataset, minimizing associated errors.

Feeding in the values from table 11, the diffusion coefficient was found to be

$$D_{\text{SanPedro}} = 4.2359 \times 10^{-17} m^2/s$$

Again, we perform a root mean square error analysis (RMSE) on the dataset to match our model and obtain the best-fit value for the diffusion time. From table 11 and Fig. 14, we obtain the diffusion time

$$t_{\text{SanPedro}} = 57.0833 \pm 0.0001 \text{ days}$$

Table 11: Parameters for SanPedro dataset [4, 5].

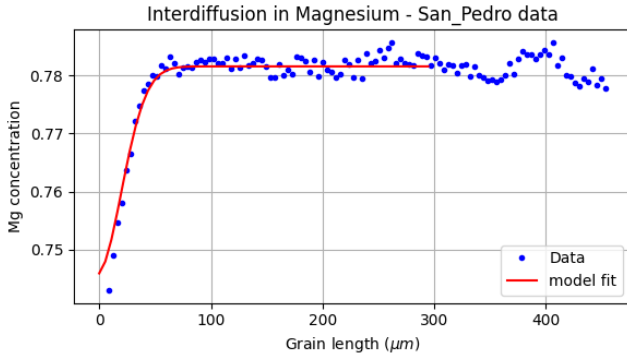| Parameters | Values |
|---|---|
| Total length of grain | $300\mu m$ |
| $L_1$ (Mg side) | $21\mu m$ |
| $L_2$ (Fe-Mg mixed side) | $279\mu m$ |
| $dt$ | 5 hrs |
| $dx$ | $1\mu m$ |
| Length offset | $30\mu m$ |
| Temperature | $1083\ °C$ |
| $\log[f(O_2)]$ | -10.37033 bars |
| Pressure | $2 \times 10^8$ bars |
| $X_{\text{Fe}}$ | 0.22 |



Figure 14: Variation of concentration of Magnesium with grain length in natural sample SanPedro

## 5 Discussion

Diffusion is a fundamental process that underlies a myriad of phenomena in nature, including the mixing of substances, chemical reactions, and the transport of materials in biological systems. In section 3, we demonstrated heat diffusion in a metal rod initially heated up to some arbitrary temperature and allowed to cool. We also showed the diffusion for different initial and boundary conditions. Additionally, we showed heat diffusion for two rods, which were initially heated to some arbitrary temperature and then joined together, keeping their extreme ends isolated. The results obtained were shown in a contour plot.

In section 4, we modeled the interdiffusion of forsterite grains for the diffusion of Fe atoms into Mg compartment. We used four laboratory datasets from [1] to calculate the optimum diffusion coefficients that matches the observed trends. Using them, the activation energy and absolute diffusion coefficient were calculated.

In section 4.3, we calculated the diffusion coefficient using the relation given in [5] and used it to investigate

the total diffusion time of the grain. These results describe that the samples had undergone the active stage of the Mt. Etna volcano 56.5 days for the Ol6a sample and 91 days for the Ol6b sample before the eruption, while the San Pedro sample had undergone the active stage 57 days before the volcanic eruption.

We report that the results obtained are in good agreement with the reference values in [1], [4, 5]. The discrepancies can be accounted for the pressure variations, $X_{\text{Fe}}$ concentration variations, and errors while taking data.

## Acknowledgements

## References

[1] Sumit Chakraborty. Rates and mechanisms of fe-mg interdiffusion in olivine at 980°–1300° c. *Journal of Geophysical Research: Solid Earth*, 102(B6):12317–12331, 1997.

[2] Fidel Costa and Sumit Chakraborty. Decadal time gaps between mafic intrusion and silicic eruption obtained from chemical zoning patterns in olivine. *Earth and planetary science letters*, 227(3-4):517–530, 2004.

[3] Fidel Costa, Thomas Shea, and Teresa Ubide. Diffusion chronometry and the timescales of magmatic processes. *Nature Reviews Earth & Environment*, 1(4):201–214, 2020.

[4] Ralf Dohmen, Hans-Werner Becker, and Sumit Chakraborty. Fe–mg diffusion in olivine i: experimental determination between 700 and 1,200 c as a function of composition, crystal orientation and oxygen fugacity. *Physics and Chemistry of Minerals*, 34:389–407, 2007.

[5] Ralf Dohmen and Sumit Chakraborty. Fe–mg diffusion in olivine ii: point defect chemistry, change of diffusion mechanisms and a model for calculation of diffusion coefficients in natural olivine. *Physics and Chemistry of Minerals*, 34(6):409–430, 2007.

[6] Maren Kahl, Sumit Chakraborty, Fidel Costa, and Massimo Pompilio. Dynamic plumbing system beneath volcanoes revealed by kinetic modeling, and the connection to monitoring data: An example from mt. etna. *Earth and Planetary Science Letters*, 308(1-2):11–22, 2011.

[7] Horton E Newsom. Composition of the solar system, planets, meteorites, and major terrestrial reservoirs. *Global earth physics: a handbook of physical constants*, 1:159, 1995.